6. Yu. A. Buyevich and I. N. Shchelchkova, Prog. Aerospace Sci., 18, No. 2, 121-150 (1978).
7. Yu. A. Buevich, Yu. A. Korneev, and I. N. Shchelchkova, Inzh.-Fiz. Zh., 30, No. 6, 979-985 (1976).
8. Yu. A. Buevich and A. Yu. Zubarev, Inzh.-Fiz. Zh., 50, No. 3, 434-445 (1986).
9. J. Happel and G. Brenner, in: Hydrodynamics at Low Reynolds Numbers [Russian translation], Moscow (1976).
10. R. Christensen, in: Introduction to the Mechanics of Composites [Russian translation], Moscow (1982).
11. L. D. Landau and E. M. Lifshits, Theoretical Physics. Vol. VI. Hydrodynamics [in Russian], Moscow (1986).
12. Yu. A. Buevich and A. Yu. Zubarev, Rheophysics of Polymeric and Disperse Liquids [in Russian], Minsk (1986), pp. 99-110.
13. B. Khuzhaerov, Inzh.-Fiz. Zh., 56, No. 1, 134-135 (1989). Submitted to VINITI 09.08.88, Reg. No. 6373—B 88.

EXPERIMENTAL STUDY OF HEAT TRANSFER FROM THE WALLS OF A CHANNEL TO A CIRCULATING FLUIDIZED BED

A. P. Baskakov, V. K. Maskaev,
I. V. Ivanov, and A. G. Usol'tsev

UDC 621.1:66.02

Results are presented from an experimental study of external heat transfer in a circulating fluidized bed.

Due to the intensive mixing of the dispersed material and the gas and the possibility of controlling their time of contact within a broad range of values, it has been found expedient to use circulating fluidized beds in a number of chemical processes and operations involving drying and combustion. The broader use of such systems is being held up by a lack of reliable data on their aerodynamics and heat transfer characteristics.

An experimental study of external heat transfer in a circulating bed was conducted on a unit at the S, M. Kirov Ural Polytechnic Institute [1]. The unit was closed with regard to the dispersed material and open with regard to the gas. The main component of the unit was a channel made of a steel tube with an inside diameter of 250 mm. The tube was composed of 10 sections placed on top of one another. The length of each section was 950 mm. Transparent windows for visual observation were located in each section. The lowest section of the channel had a gas-distributing grate with a through section of 10%. The grate functioned as an aerodynamic chamber in the given set-up. The finely dispersed material was quartz sand with a mean-mass particle diameter of 287 μm. The fractional composition of the sand is shown in Table 1.

The bulk and true densities of the sand were 1249 and 2640 kg/m^3. In amounts of up to 12.1 tons/h (which corresponded to a change of up to 70 kg/(m^2·sec) in the unit load of material per 1 m^2 of channel cross section), the solid phase was introduced into the unit with the use of a cantilever-type screw feeder with an inside diameter of 144 mm. The feeder was positioned 175 mm above the grate. The delivery of air into the feeder kept it from becoming obstructed in the case of high sand feeds. The bed was fluidized with air having a temperature of 30-60°C. The air was directed through the grate with a filtration velocity w ranging from 5 to 10 m/sec (calculated on the basis of the empty cross section of the channel). Here, the theoretical eddy velocity of the particles was 3.4 m/sec for particles 0.4 mm in diameter and 6 m/sec for particles 0.8 mm in diameter. At the outlet of the channel, the disperse flow was separated in a two-stage dust separator consisting of cyclones and a bag filter. Passing through a system of hoppers and shut-off valves, the particles returned to the air chamber, while the air was released into the atmosphere.

Ural Polytechnic Institute, Sverdlovsk. Translated from Inzhenerno-Fizicheskii Zhurnal, Vol. 59, No. 6, pp. 975-979, December, 1990. Original article submitted January 24, 1990.

 0022-0841/90/5906-1570$12.50

TABLE 1. Fractional Composition of the Quartz Sand

Size of fraction, mm		Mass content, %
upper	lower	
	0,8	0,025
0,8	0,63	0,02
0,63	0,4	24,25
0,4	0,315	16,9
0,315	0,25	12,57
0,25	0,2	9,76
0,2	0,16	5,58
0,16	0,1	0,92
0,1	0,08	13,82
0,08	0,063	3,8
0,063	0,05	1,88
0,05	0,04	2,94
0,04	Дно	7,535

External heat transfer in the circulating fluidized bed was studied by a steady-state method on an experimental section (Fig. 1) consisting of four annular copper transducers 100 mm long. The inside diameter of the transducers was 0.25 m, which was equal to the diameter of the channel of the unit. An electric heater made of nichrome wire was wound about each transducer. The power of the heater was regulated with the aid of a laboratory auto-transformer. The outside surface of the heater was enveloped with a layer of thermal insulation made of kaolin wool. Thermocouples were caulked into the middle and the ends of each transducer. The thermocouples were also used to measure the temperature drop through the thickness of the insulation and the temperature of the circulating bed. The coefficient of heat transfer between the bed and each transducer was calculated from the power of the heaters with allowance for heat loss from the outer surface of the insulation and through the ends after attainment of the steady-state regime. The transducers in the above-described set-up could be connected either individually or in combination.

In the expriments we conducted, the distance from the gas-distributing grate to the middle of the measurement section (with a total length of 0.4 m) was 0.6, 1.04, 4.88, and 7.77 m.

Figure 2 shows the results of evaluation of the accuracy of the method in experiments conducted with just air. Accuracy was evaluated by comparing the results of these experiments with results calculated from the empirical formula

$$\overline{\mathrm{Nu}}_D = 0{,}0214\,(\mathrm{Re}_D^{0,8} - 100)\,\mathrm{Pr}^{0,4}\left[1 + \left(\frac{D_t}{l}\right)^{2/3}\right], \qquad (1)$$

presented in [2] for approximately analogous conditions. The satisfactory agreement between the theoretical (straight line) and experimental (points) data indicates the reliability of the method. It follows from the formula that the coefficient of heat transfer α_a to the dust-free air depends on the diameter and length of the transducer but is independent of the height of its installation in the channel. This is confirmed by the experimental data (dashed lines in Fig. 3). The value of α_a of course increases with an increase in air velocity.

Figure 3 shows the change in the heat-transfer coefficient $\bar{\alpha}$ over the height of the experimental channel with different fluidization velocities and different sand loads. The coefficient turned out to be roughly the same at elevations of 7.77 and 4.88 m, while it increased sharply on the acceleration section, going toward the grate. It is difficult to explain the small decrease in $\bar{\alpha}$ at a height of 0.6 m with a velocity of 5.2 m/sec and $G_s >$ 18 kg/(m^2·sec). The heat-transfer coefficient $\bar{\alpha}$ increased at all elevations with an increase in the unit load. In certain regimes, a small increase in $\bar{\alpha}$ was seen on the outlet section. This was particularly the case at velocities on the order of 10 m/sec and G_s = 40-70 kg/(m^2·sec).

The above patterns are the result of the aerodynamics of the circulating fluidized bed and, most of all, the distribution of particle concentration over the height of the unit. As in tests conducted with aluminum hydroxide [1], the density of the bed is nearly constant

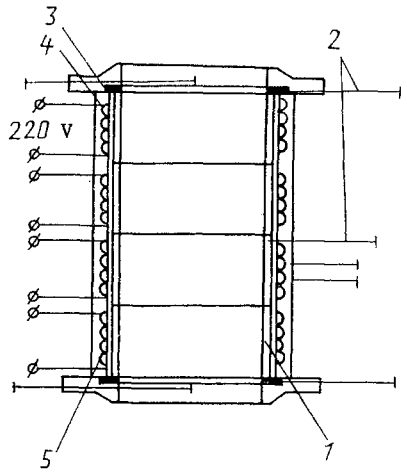

Fig. 1

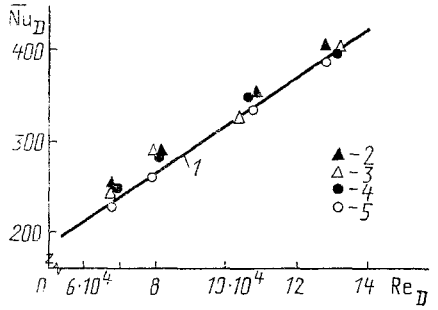

Fig. 2

Fig. 1. Sketch of measurement section: 1) annular copper transducer; 2) thermocouple; 3) electrical insulation; 4) thermal insulation; 5) electric heater.

Fig. 2. Effect of the turbulence of a dust-free flow of air on the corrected heat-transfer coefficient at different heights above the gas-distributing grate: 1) calculation from (1); 2) H = 0.6 m; 3) 1.04; 4) 4.88; 5) 7.77.

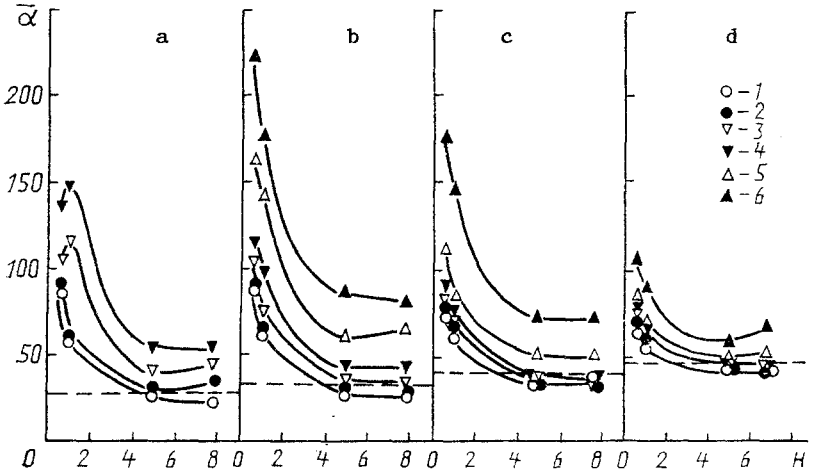

Fig. 3. Change in the mean heat-transfer coefficient over the height of the experimental channel with different unit loads and velocities of fluidizing air: a) w = 5.2 m/sec; b) 6.1; c) 8.2; d) 10.1; 1) G_S = 9.5 kg/(m²·sec); 2) 12.7; 3) 18.3; 4) 27.5; 5) 41.4; 6) 68.7 (dashed line — pure air). $\bar{\alpha}$, W/(m²·K); H, m.

at elevations greater than roughly 4 m. Below this level, density progressively increases as the grate is approached. The correspondence between the heat-transfer coefficient and density is also seen in the above-mentioned increase in density in the top part of the unit — where particle concentration increases due to eddying of the flow associated with its abrupt rotation.

In the case of low bed density, the relationship between these quantities is nonmonotonic. Thus, with an increase in G_S from zero to 10-20 kg/(m²·sec), the heat-transfer coefficient in the upper part of the unit (at H = 4.88 and 7.77 m) decreases by 10-15% compared to the heat transferred to the dust-free air. This occurs despite the increase in particle concentration. The deterioration in heat transfer is evidently due to the extinction of turbulent pulsations and redistribution of the velocity profile when the solid phase is introduced into the channel. A further increase in the unit load is accompanied by a substantial increase in the heat-transfer coefficient. Meanwhile, the lower the velocity of air,

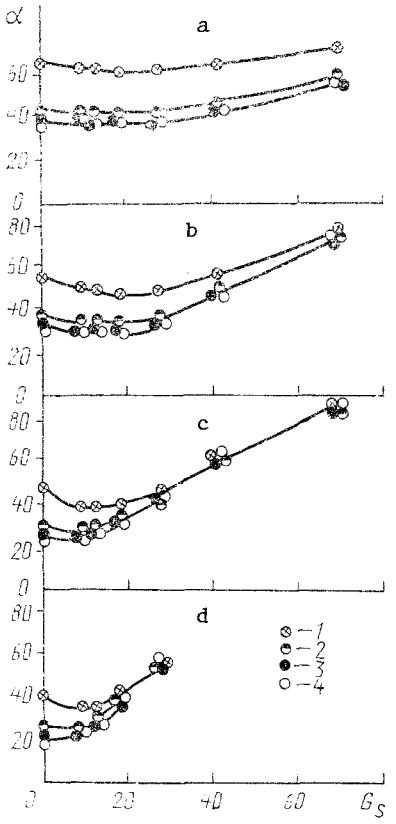

Fig. 4. Change in the local heat-transfer coefficient over elements of the measurement section located at height H = 4.88 m above the gas-distributing grate in relation to the unit load and the velocity of the fluidizing air: a) w = 10.1 m/sec; b) 8.2; c) 6.1; d) 5.2; distance from the grate to the elements of the section: 1) h = 4.73 m, 2) 4.83; 3) 4.93; 4) 5.03. α, W/(m²·K); G_S, kg/(m²·sec).

the more intensive the increase in $\bar{\alpha}$. This outcome has to do with the removal of heat from the transducer by the particles themselves.

An increase in velocity is accompanied by an increase in the coefficient of heat transfer to the pure air and, accordingly, by a decrease in the coefficient of heat transfer $\bar{\alpha}$ to the dust-laden flow. However, the corresponding unit loads increase in the latter case. In the case of a small unit load, rectilinear streamline motion of the particles is observed visually. With an increase in G_S, this becomes motion in which strands of particles infrequently "stick" to the walls. The walls are poorly washed by the particles, with the "attached" strands sometimes moving downward and being separated by the ascending flow. With a further increase in G_S, we observed alternating upward and downward motion of the strands and eddies and momentary "attachment." With an even greater increase in the unit load, we saw mainly downward motion of particle strands along the walls and momentary attachment; the strands were sometimes separated from the walls by the ascending flow. At the maximum load, there was intensive downward motion of the particles in the form of jets, eddies, and a continuous flow, while upward motion was absent. The higher the air velocity, the higher the unit loads corresponding to the transition from one flow pattern to another. The minimum of the heat-transfer coefficient corresponded to a transition from rectilinear ascent of the particles to alternating upward-downward motion at all air velocities.

At distances from the grate equal to 0.6 and 1.04 m, no decrease in the heat-transfer coefficient with an increase in the unit load of particles was seen due to the higher bed density for the same values of G_S and, thus, the higher value of the heat-transfer coefficient (Fig. 3).

Figure 4 shows values of the heat-transfer coefficients for each of four calorimeter elements installed 4.88 m above the grate. In the case of heat transfer with a dust-free flow, a thermal boundary layer was formed on the calorimeter surface. The thickness of this layer increased down the flow. Thus, the heat-transfer coefficient from the lower element turned out to be the highest, while the same coefficient from the higher element was the lowest. The contribution of the particles became more significant as their concentration was increased and, at a certain value of G_S (~20 kg/(m^2·sec) with w = 5.2 m/sec or 30 kg/(m^2·sec) at w = 6.1 – see Fig. 4), the boundary layer (in the sense of the term used above) disappeared; the coefficient of heat transfer from all of the calorimeter elements turned out to be the same. It can be seen from Fig. 4 that air convection has a greater effect, the higher the velocity of air. At w = 8.2 m/sec and especially at w = 10.1 m/sec, it is markedly greater even for the limiting value G_S = 70 kg/(m^2·sec) achieved in the experiment.

It follows from the above that the mechanism of external heat transfer in a circulating fluidized bed is quite complex and that a more detailed study will be required to investigate its different aspects.

NOTATION

D_t, diameter of tube, m; G, mass flow rate of dispersed material; $G_S = G/S$, unit load of dispersed material, kg/(m^2·sec); h, distance from gas-distributing grate to middle of measurement section, m; ℓ, length of heat-transfer section, m; $Nu_D = \alpha D_t/\lambda$, Nusselt number describing external heat transfer in the tube; $Re_D = wD_t/\nu$, Reynolds number; Pr, Prandtl number; S, cross section of channel, m^2; w, filtration velocity of gas, calculated on the basis of the empty cross section of the channel, m/sec; α, coefficient of heat transfer from the tube wall, W/(m^2·K); λ, thermal conductivity, W/(m·K); ν, kinematic viscosity, m^2/sec. Indices: a, dust-free air; t, tube; superimposed bar denotes mean value.

LITERATURE CITED

1. V. K. Maskaev, A. P. Baskakov, A. G. Usol'tsev, and I. V. Ivanov, Inzh.-Fiz. Zh., 57, No. 5, 762-767 (1989).
2. B. S. Petukhov and V. N. Shikov (eds.), Handbook of Heat Exchangers [Russian translation], Vol. 1, Moscow (1987).